

Fermi Liquid Theory and Ferromagnetic Manganites at Low Temperatures

M. O. Dzero¹, L. P. Gor'kov^{1,2} and V. Z. Kresin³

¹*National High Magnetic Field Laboratory, Florida State University, Tallahassee, FL 32310*

²*L.D. Landau Institute for Theoretical Physics, Russian Academy of Sciences, 117334 Moscow, Russia*

³*Lawrence Berkeley Laboratory, University of California, Berkeley, CA 94720*

(May 20, 2021)

Fermi liquid characteristics for ferromagnetic manganites, $A_{1-x}B_xMnO_3$, are evaluated in the tight-binding approximation and compared with experimental data for the best studied region $x \simeq 0.3$. The bandwidths change only slightly for different compositions. The Sommerfeld coefficient, γ , the T^2 -term in resistivity and main scales in optical conductivity agree well with the two band model. The “2.5” - transition due to a “neck” forming at Fermi surface, is found at $x = 0.3$. The mean free path may change from 3 to 80 interatomic distances in the materials, indicating that samples’ quality remains a pressing issue for the better understanding of manganites.

PACS numbers: 72.15.Gd, 75.30.Ds

Experiments on doped “pseudocubic” manganites, $A_{1-x}B_xMnO_3$, primarily engendered by prospects of applications of the “colossal” magnetoresistance (CMR) effect, unveiled unexpected richness of new phenomena pressing for a fundamental interpretation (for review see, e.g.^{1,2}). The consensus is that the “double exchange” (DE) mechanism³, together with the Jahn-Teller (JT) instability of the degenerate e_{2g} -term at the Mn^{3+} -site pre-determine the (x, T) -phase diagram of the low doped manganites. The one-electron Hamiltonian of the form⁴:

$$\hat{H} = \sum_{i,\delta} (\hat{t}_{i,i+\delta} - J_H(\mathbf{S}_i \cdot \hat{\sigma}) + g\hat{\tau} \cdot \mathbf{Q}_i + J_{def}\mathbf{Q}_i^2) \quad (1)$$

accounts for the competition between the first two terms in (1) ($\hat{t}_{i,\delta}$ being a tunneling matrix, while J_H is the strong intrasite Hund’s coupling) which, in accordance with the DE-mechanism, tend to form ferromagnetic electronic bands, and localizing effects of the thermal disorder in the JT-degrees of freedom (the last two terms). The method⁴ interpolates the high- and low-temperature regimes in “low doped” ($x < 0.5$) manganites in terms of crossover between “small” and “large” polarons conduction⁴⁻⁶. It is not apt to draw conclusions regarding the ground state symmetry.

Another issue is whether the electron-electron interactions are of principle importance for manganites. The stoichiometric compound, $LaMnO_3$, is an antiferromagnetic (the A-phase) insulator and preserves the insulating low-T behavior even at doping, x , below $x_{cr} \simeq 0.16 - 0.17$. These features are often treated in the literature in terms of a Mott-Hubbard state. It has been demonstrated in⁷ that properties of $LaMnO_3$ may be easily rationalized in terms of the band insulator provided static JT-distortions are taken into account in the electron band structure. It was also argued that the critical concentration $x_{cr} \simeq 0.16 - 0.17$ for the onset of a metallic (low T) conductivity is precisely the percolation threshold. (The CMR-phenomenon at T_c itself may be interpreted in the percolative terms as well⁸). Hence, at x close enough to x_{cr} doped manganites exist as a

highly inhomogeneous “mixture” of tiny islands of co-existing phases of a size, limited by the Coulomb forces (typically, of the order of $10-20 \text{ \AA}$ ^{9,10}). Crossover from percolation regime to homogeneous ferromagnetic phase seems to take place below $x \sim 0.3$ (see discussion below). In what follows we analyze available low temperature experimental data for doped manganites with $x \sim 0.3$.

As x increases above x_{cr} , percolation, being a critical phenomenon, may cede soon to the onset of the homogeneous ferromagnetic phase, when screening becomes effective. In fact, some good samples of $La_{1-x}Sr_xMnO_3$ show low temperature resistivity in the range $10^{-4} - 10^{-5}(\Omega - cm)$ ¹¹.

In what follows we analyze available low temperature experimental data for doped manganites from this point of view. Our conclusions are that the band model (or Fermi liquid) approach gets valid at low temperatures, especially for high quality samples. Data are hindered by sample’s quality with local inhomogeneities forming scattering centers. For a number of compositions depending on tolerance factor, conductivity is close to it’s value in the mobility edge regime. Data on low frequency optical conductivity $\sigma(\omega)$ ($\omega < 1eV$) remain a controversial issue (at low T), although agree qualitatively with the two band model⁷.

Summary of the Theoretical Results. – We adopt the model and notations of⁷. The electron spectrum consists of the two branches:

$$\varepsilon_{\pm}(\mathbf{p}) = -|A| \cdot (c_x + c_y + c_z \pm R(\mathbf{p})), \quad (2)$$

$$R(\mathbf{p}) = \sqrt{c_x^2 + c_y^2 + c_z^2 - c_x c_y - c_x c_z - c_y c_z}. \quad (3)$$

Here for brevity: $c_i = \cos \tilde{p}_i$, $\tilde{p}_i = p_i a$.

We calculate the concentration dependence of the Fermi-level, $E(x)$, the density of states (DOS), $\nu(x)$, the spin stiffness, $D(x)$, and the whole magnon spectrum, $\omega(\mathbf{k}, x)$, and the conductivity, $\sigma(\omega, x)$, both the Drude and the optical (interband) components. Theoretical results depend only on the single hopping integral, $|A|$. In addition, for the stoichiometric $LaMnO_3$ the optical data

for $\sigma(\omega)$ at $x = 0^{15,16}$ allow to evaluate the electron coupling with the JT-distortions.

To find the spin waves spectrum, present deviations from the average spin, $\langle S_z \rangle$ for the localized t_{2g} -spins ($\mathbf{s} = \mathbf{S} - \langle S_z \rangle$) as:

$$\begin{aligned} s^+(\mathbf{q}) &= (2\langle S_z \rangle)^{1/2} \hat{b}(\mathbf{q}), \quad s^-(\mathbf{q}) = (2\langle S_z \rangle)^{1/2} \hat{b}^+(\mathbf{q}), \\ s_z(\mathbf{q}) &= (\hat{b}^+ \hat{b})_{\mathbf{q}}, \end{aligned} \quad (4)$$

(\hat{b}^+, \hat{b} -the magnon's operators). The first (δE_1) and second (δE_2) order corrections to the ground state are calculated as perturbations in:

$$\hat{V} = -J_H \sum_i \mathbf{s}_i (\hat{a}_i^+ \sigma \hat{a}_i) = -J_H \sum_i \mathbf{s}_i \mathbf{n}_i. \quad (5)$$

For δE_2 , the matrix elements in (5) are of the form:

$$\begin{aligned} V_{\mathbf{p}-\mathbf{k}, \uparrow; \mathbf{p} \downarrow}^{l, l'} &= -J_H \langle \uparrow | s^\pm(\mathbf{k}) | \downarrow \rangle \times \\ &\times \left(\alpha_{\mathbf{p}-\mathbf{k}}^l \alpha_{\mathbf{p}}^{*l'} + \beta_{\mathbf{p}-\mathbf{k}}^l \beta_{\mathbf{p}}^{*l'} \right), \end{aligned} \quad (6)$$

(see (9)). As for δE_1 , its only role is to secure the proper behavior of the magnon spectrum at $k \rightarrow 0$). One obtains:

$$\begin{aligned} \delta E_2 &= 2J_H^2 \sum_{\mathbf{k}} \langle S_z \rangle \hat{b}^+(\mathbf{k}) \hat{b}(\mathbf{k}) \times \\ &\times \sum_{l, \mathbf{p}} \left(\sum_{l'} \frac{|\alpha_{\mathbf{p}}^l \alpha_{\mathbf{p}+\mathbf{k}}^{*l'} + \beta_{\mathbf{p}}^l \beta_{\mathbf{p}+\mathbf{k}}^{*l'}|^2}{E_{\uparrow}^l(\mathbf{p}) - E_{\downarrow}^{l'}(\mathbf{p}+\mathbf{k})} \right), \end{aligned} \quad (7)$$

where

$$E_{\uparrow, \downarrow}^{l, l'}(\mathbf{p}) = \mp J_H \langle S_z \rangle + \varepsilon_{l, l'}(\mathbf{p}). \quad (8)$$

Both sums in (7) run over $l, l' = \pm$ (Eq.(2)). The summation over l and \mathbf{p} is limited by the occupied states (\uparrow) only. The coefficients ($\alpha_{\mathbf{p}}^l, \beta_{\mathbf{p}}^l$) above are for the Bloch's states on the basis, used in⁷:

$$\alpha_{\mathbf{p}}^{l, l'} = (t_{12}/2|t_{12}|)^{1/2}, \quad \beta_{\mathbf{p}}^{l, l'} = \pm (t_{21}/2|t_{12}|)^{1/2}, \quad (9)$$

(here t_{12}, t_{21} are the off-diagonal elements of the hopping matrix $\hat{t}(\mathbf{p})$ in (1) on this basis).

Assuming in (7, 8) $J_H \gg |A|$ ($J_H \langle S_z \rangle$ is of the order of 1.5 eV^1 , estimates below produce for $|A| \sim 0.1 \text{ eV}$), expansion (7) in $|A|/J_H$ gets equivalent to the series of the Heisenberg spin Hamiltonians accounting for interactions with the increasing number of neighbors. (For a single band it was first noticed in¹⁷). In the two band model⁷ the first order term in $|A|$ from (7) is ($\langle S_z \rangle = 3/2$):

$$\hbar\omega(\mathbf{k}) = |A|(3 - c_x - c_y - c_z)D(x)/3 \quad (10)$$

and $D(x) \equiv D(E(x))$ is given by the integral:

$$\int \frac{d^3\mathbf{p}}{(2\pi)^3} \left[\sum_{(+,-)} \theta(E - \varepsilon_i(\mathbf{p})) \left\{ 1 \pm \frac{2c_x - c_y - c_z}{2R(\mathbf{p})} \right\} \right],$$

(here E is in units of $|A|$, $p_i \equiv ap_i$). Quantum fluctuations may change the \mathbf{k} -dependence in Eq. (10).

To calculate the conductivity, $\sigma(\omega, x)$, we determine first the velocity operator, $\hat{\mathbf{v}} = \dot{\hat{\mathbf{r}}}$ (see¹⁸):

$$\hat{\mathbf{v}}(\mathbf{k}) = \frac{1}{\hbar} \frac{\partial \varepsilon_l(\mathbf{k})}{\partial \mathbf{k}} + \frac{i}{\hbar} [\varepsilon_l(\mathbf{k}) - \varepsilon_{l'}(\mathbf{k})] \langle l\mathbf{k} | \hat{\Omega} | l'\mathbf{k} \rangle. \quad (11)$$

The off-diagonal operator $\hat{\Omega}$ is defined by the relation:

$$\langle l\mathbf{k} | \hat{\Omega} | l'\mathbf{k} \rangle = i \int u_{\mathbf{k}}^{*l'}(\mathbf{r}) \frac{\partial u_{\mathbf{k}}^l}{\partial \mathbf{k}} d^3\mathbf{r} \quad (12)$$

and $u_{\mathbf{k}}^l(\mathbf{r})$, the periodic Bloch functions on the basis⁷ are:

$$\begin{aligned} u_{\mathbf{k}}^l(\mathbf{r}) &= \frac{1}{\sqrt{N}} \sum_n \exp[i\mathbf{k}(\mathbf{a}n - \mathbf{r})] \times \\ &\times \{ \alpha_{\mathbf{k}}^l \phi_1(\mathbf{r} - n\mathbf{a}) + \beta_{\mathbf{k}}^l \phi_2(\mathbf{r} - n\mathbf{a}) \}. \end{aligned} \quad (13)$$

With the one-site integrals only in (12) and Eqs. (9):

$$\langle l\mathbf{k} | \hat{\Omega} | l'\mathbf{k} \rangle = i \frac{a}{\hbar} \frac{\sqrt{3}}{4} \frac{(-\sin k_x)(c_y - c_z)}{|t_{12}|^2}. \quad (14)$$

Eqs. (11, 14) produce transitions from *occupied* parts of the $\varepsilon_+(\mathbf{p})$ -band into *empty* states in the $\varepsilon_-(\mathbf{p})$ -band.

With all the above, we arrive to the Drude (intraband) contribution which in the clean limit is:

$$\sigma_{Drude}(\omega, x) = 2\pi \frac{e^2 |A|}{3a\hbar^2} \delta(\omega) I_{Dr}(x), \quad (15)$$

$$I_{Dr}(x) = \frac{1}{2(2\pi)^3} \sum_l \int dS_{\mathbf{p}} |\nabla_{\mathbf{p}} \varepsilon(\mathbf{p})|, \quad (16)$$

(the integral in $I_{Dr}(x)$ is over the Fermi surfaces (FS)). The "optical" (interband) contribution is

$$\begin{aligned} \sigma_{opt}(\omega, x) &= \frac{3\pi e^2}{a\hbar} \frac{1}{\tilde{\omega}_0^3} \int \frac{d^3\mathbf{p}}{(2\pi)^3} \sin^2 p_x (c_y - c_x)^2 \times \\ &\times n(\varepsilon_+(\mathbf{p})) [1 - n(\varepsilon_-(\mathbf{p}))] \cdot \delta(\tilde{\omega} - 2R(\mathbf{p})), \end{aligned} \quad (17)$$

where $|A|\tilde{\omega} = \hbar\omega$ (Eqs. (16) and (17) agree with the results of¹⁹). For the low temperature spectral weights

$N_{eff} = \frac{2m}{\pi e^2} a^3 \int_0^\infty \sigma(\omega) d\omega$, one obtains for the Drude and the interband contributions, respectively:

$$N_{eff}^{Drude} = \frac{ma^2}{3\hbar^2} |A| I_{Dr}(x), \quad N_{eff}^{opt} = \frac{ma^2}{\hbar^2} |A| \frac{3}{4} I_{opt}(x), \quad (18)$$

(with $I_{opt}(x)$ directly obtained from (17)). In Fig. 1 we plotted our results for the Fermi level, $E_F(x) = |A|E(x)$, $\tilde{\nu}(x) = \nu(x)|A|$, $D(x)$ and $I_{Dr}(x)$. In Fig. 2 the Fermi surface at $x=0.3$ is shown (the shaded area shows schematically the concentration range for a percolative regime).

Fermi Liquid and the Experimental Data.— We choose to determine the band parameter, $|A|$, from measurements of the spin stiffness coefficient: $\hbar\omega(\mathbf{k}) =$

$(\mathbf{k}a)^2|A|D(x)/6$. As the long-wave characteristics, $D(x, T=0)$ is less sensitive to a samples' disorder. We use $a \simeq 3.86\text{\AA}$, $D(x \simeq 0.3) \simeq 0.45$ and data in¹⁴ (Table 1). The results for $|A|$ show that the bandwidths for different materials, $W=6|A|$, do not vary significantly (0.7 – 1.0 eV) as if changes in the Mn-O-bond angle in different materials are *not* of importance. The differences in ionic radii regulate mainly the local disorder as seen from data on resistivity (see below). According to²³, $D(x)$ first increases with x above x_{cr} and saturates at $x \sim 0.3$. The initial increase of $D(x)$ ²³ merely reflects the fact that above the percolation threshold the percentage of the FM-phase increases (magnetic moment increases). In the FM-phase further increase in x leads to *decrease* of the magnetization and $D(x)$ in Fig. 1 decreases. This decrease is beyond the accuracy of data²³, and the crossover into FM state is seen as a saturation of $D(x)$ at $x = 0.28, 0.3$ ²³.

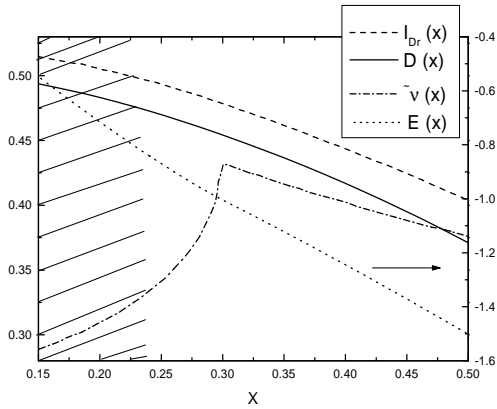


FIG. 1. The Fermi level, $E(x)$, DOS, $\tilde{\nu}(x)$, the spin stiffness coefficient $D(x)$ and the Drude conductivity, $I_{Dr}(x)$, plotted as a function of concentration, x , for the spectrum Eq. (2). The shaded area shows the percolative regime where Eqs. (9-18) are not applicable.

Another important parameter, the Sommerfeld coefficient, γ , for our spectrum (2) is:

$$\gamma = \pi^2 \tilde{\nu}(x) / 3|A|. \quad (19)$$

Eq. (19) gives $\gamma \sim 6.2 \text{ mJ/mole}\cdot\text{K}^2$ ($\tilde{\nu}(x) \sim 0.45$ at $x \simeq 0.3$). According to²⁰, $\gamma \simeq 3.5 \text{ mJ/mole}\cdot\text{K}^2$ for $\text{La}_{0.7}\text{Sr}_{0.3}\text{MnO}_3$. The low-T heat capacity of a few other manganites with compositions $x \simeq 0.3$ has been measured with γ in the 3-8 $\text{mJ/mole}\cdot\text{K}^2$ range¹.

For most of experimental results it is common (e.g.^{1,20}) to “separate” the $T^{3/2}$ magnon term in the specific heat. Here lies an interesting catch. Namely, close to $x=0.3$ in addition to that of magnons, there is the *band* $T^{3/2}$ -contribution into the specific heat. Indeed, the Fermi surface in Fig. 2, shows a formation of the “neck” at the zone boundary very close to $x = 0.3$, and, hence, this is the point of the “2.5”-Lifshitz transition! With this in mind, one should recognize a rather good agreement

between (19) and the low-T experimental data on the heat capacity. As it is easy to see, $\tilde{\nu}(x)$ in Fig. 1 varies significantly near $x=0.3$.

Substitution of divalent atoms at such concentrations inevitably leads to intrinsic disorder. It is argued in⁹ that this disorder, seen in $\text{La}_{1-x}\text{Sr}_x\text{MnO}_3$ even at $T=10 \text{ K}$ at $x < 0.35$ is mainly due to the local JT-distortions and bears a quasistatic character at $x > 0.17$. Part of carriers may be trapped into the JT polarons, forming the microdomains of an insulating phase. The disorder is a factor, which may affect our interpretation. In view that resistivities for samples with nominally the same concentration may differ in the order of magnitude, it is essential to evaluate related spatial and energy scales. We substitute in Eq.(16) $\pi\delta(\omega) \rightarrow \tau/(1 + (\omega\tau)^2)$ to obtain the effective \hbar/τ due to residual resistivities. This gives $\hbar/\tau|A| \sim 0.5$ for materials with $\rho \simeq 300(\mu\Omega - \text{cm})$, but it is only $\sim 2 \cdot 10^{-2}$ for the film samples of $\text{La}_{0.7}\text{Sr}_{0.3}\text{MnO}_3$ ⁶. With the average velocity of an electron on the FS in our model $\langle v^2 \rangle^{1/2} = (|A|a/\hbar) (2I_{Dr}(x)/\tilde{\nu}(x))^{1/2}$, the mean free path, l , is typically of the order of $l \sim 3a$ for most samples, while $l \sim 80a$ is reached in the best LSMO-samples⁶. It remains to be seen whether sample's quality may be further improved.

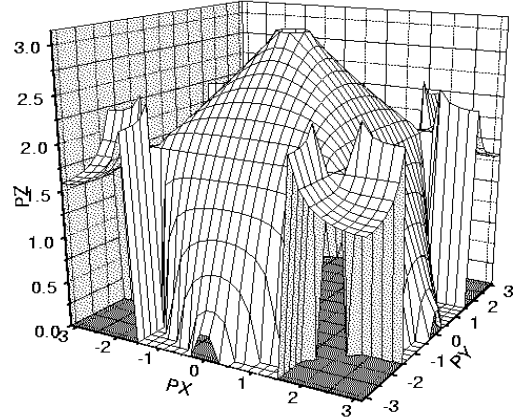


FIG. 2. The FS at $x \approx 0.3$. “Necks” forming at the zone boundary are responsible for singularity in $\tilde{\nu}(x)$ in Fig. 1.

The T^2 – term in resistivity due to the electron interactions comes from $\hbar/\tau_{ee}^{tr} = \lambda'(\hbar/\tau_{ee})$, where τ_{ee} is the total quasiparticle relaxation time and $\lambda' < 1$ gives the fraction of Umklapp processes. We use²¹:

$$\hbar/\tau_{ee} \simeq \lambda\pi^3\nu(x)T^2. \quad (20)$$

In (20) λ is a value of the interaction strength in terms of E_F . Using^{6,11}, one obtains for LSMO: $\lambda\lambda' \simeq 0.3$, typical of good metals. As for the two other materials in⁶, the T -variations of resistivity scale in the magnitude with their residual resistivity and are caused by defects²².

T -dependence in the optical conductivity, $\sigma(\omega)$, at-

tracted recently much attention^{6,16,20} as a manifestation of changes in the conductivity mechanism at elevated temperatures. We discuss only a few results pertinent to the low T band mechanisms. First note, that the temperature dependence in $\sigma(\omega)$ at $T < 100$ K for ω around 1eV is most pronounced *below* 1eV (see Fig. 2 in⁶). This agrees well with our estimates for the bandwidths, $W \leq 1$ eV. As for a quantitative analysis, there are problems of an experimental character. Assuming $N_{eff}(\omega)$ ⁶ would give our N_{eff} 's in Eq. (18) at $\omega \simeq 1$ eV and that both the Drude and optical contributions are approximately equal¹⁹, we obtain $N_{eff} \sim 0.25$ which is reasonably close to the values in⁶, lesser than N_{eff} for the single crystal data, $\text{La}_{0.67}\text{Ca}_{0.33}\text{MnO}_3$ ¹⁶, and a factor ten bigger than N_{eff} for $\text{La}_{0.7}\text{Sr}_{0.3}\text{MnO}_3$ in¹⁵. We believe that such a difference originates from poor data for the optical $\sigma(\omega)$ in the ‘‘Drude-tail’’ range.

Finally, the optical gap for pure LaMnO_3 was identified¹⁵ at $\Delta \simeq 1.2$ eV. A rough estimate from the band insulator picture⁸ gives $g \sim 0.6$ eV, i.e. the JT-coupling is rather strong ($|A| \sim 0.16$ eV).

We conclude the discussion by a few comments regarding the spin wave spectrum. In $\text{La}_{0.7}\text{Pb}_{0.3}\text{MnO}_3$ ¹² the spectrum fits well (10). Eq.(10) follows from (7) at $A \ll J_H \langle S_z \rangle$, with quantum corrections neglected. Meanwhile, strong deviations from (10) have been observed at $\xi > 0.25$ along the $(0,0,\xi)$ -direction in $\text{Pr}_{0.63}\text{Sr}_{0.37}\text{MnO}_3$ ¹³. The spin stiffness changes only slightly from material to material¹⁴, and other low temperature characteristics including electron interactions in (20), also seem not to vary much. Unlike¹⁴, we suggest with¹³ that differences in low- T spin dynamics for two materials do not correlate with their behavior at higher temperatures, but with a tendency to a low temperature charge ordering at x close to 0.5.

In conclusion, we investigated low temperature properties of different manganites with hole concentration close to $x \simeq 0.3$. Not only the tight-binding model⁷ demonstrates applicability of the Fermi liquid approach at $T \rightarrow 0$, but also it agrees with most experimental data, suggesting thus the unifying approach to ferromagnetic manganites. Bandwidths for different materials change only slightly. Concentration $x \simeq 0.3$ is remarkable for the 2.5 – topological transition. Samples quality remains a major obstacle to further elaboration of the low temperature properties. In some materials conductivity falls into the mobility edge regime.

L.P.G. and V.Z.K. gratefully acknowledge H.D. Drew, T. Egami, J. Lynn, S. von Molnar for numerous stimulating discussions. L. P. G. thanks S. Watts for essential help with some calculations. The work was supported (L.P.G. and M.O.D.) by the National High Magnetic Field Laboratory through NSF Cooperative Agreement # DMR-9527035 and the State of Florida.

- ¹ J.M.D. Coey, M. Viret, and S. von Molnar, *Adv. Phys.* **48**, 167 (1999).
- ² A.P. Ramirez, *J. Phys.: Condens. Matter* **9**, 8171 (1997).
- ³ G. Zener, *Phys. Rev.* **82**, 403 (1951); P.W. Anderson and H. Hasegawa, *Phys. Rev.* **100**, 675 (1955).
- ⁴ A.J. Millis, B.J. Shraiman, and R. Mueller, *Phys. Rev. Lett.* **77**, 175 (1996); *Phys. Rev. B* **54**, 5405 (1996).
- ⁵ H. Roder, Jun Zang, and A.R. Bishop, *Phys. Rev. Lett.* **76**, 1356 (1996).
- ⁶ M. Quijada *et al.*, *Phys. Rev. B* **58**, 16093 (1998).
- ⁷ L.P. Gor'kov and V.Z. Kresin, *JETP Lett.* **67**, 985 (1998). The idea of percolative approach to conductivity has also been brought about by D. Louca *et al.*, *Phys. Rev.* **56**, R8475 (1997), (see²⁸ in this paper).
- ⁸ L.P. Gor'kov, *Soviet. Phys.-Uspekhi* **41**, 589 (1998); L.P. Gor'kov and V.Z. Kresin, *J. Supercond.* **12**, 243 (1999).
- ⁹ D. Louca and T. Egami, *Phys. Rev. B* **59**, 6193 (1999); *J. Supercond.* **12**, 23 (1999).
- ¹⁰ M. Hennion *et al.*, *Phys. Rev. Lett.* **81**, 1957 (1998).
- ¹¹ S.E. Lofland *et al.*, *J. Appl. Phys.* **79**, 5166 (1996).
- ¹² T.G. Perring *et al.*, *Phys. Rev. Lett.* **77**, 711 (1996).
- ¹³ H.Y. Hwang *et al.*, *Phys. Rev. Lett.* **80**, 1316 (1998).
- ¹⁴ J.A. Fernandez-Baca *et al.*, *Phys. Rev. Lett.* **80**, 4012 (1998).
- ¹⁵ Y. Okimoto *et al.*, *Phys. Rev. B* **55**, 4206 (1998).
- ¹⁶ A.V. Boris *et al.*, *Phys. Rev. B* **59**, R697 (1999).
- ¹⁷ N. Furukawa, *J. Phys. Soc. Jpn.* **65**, 1174 (1996).
- ¹⁸ E.M. Lifshitz and L.P. Pitaevskii, *Statistical Physics, Part 2* (Pergamon Press, Oxford 1989) p. 227.
- ¹⁹ A. Takahashi and H. Shiba, *Eur. Phys. J.* **B5**, 413 (1998).
- ²⁰ T. Okuda *et al.*, *Phys. Rev. Lett.* **81**, 3203 (1998).
- ²¹ V. Gantmakher and Y. Levinson, *Carrier Scattering in Metals and Semiconductors* (North-Holland, Amsterdam, 1987) p. 139.
- ²² G. Mahan, *Many Particle Physics* (Plenum Press, New-York, 1993) p. 686.
- ²³ A. H. Moudden *et al.*, *Physica B* **241-243**, 276 (1998)